

Growth, characterisation and spectroscopy studies of ADP Single crystals with Se(IV)

P. Punitha^a, S. Senthilkumar^{*}

^aAssistant Professor, Department of Chemistry, Government Polytechnic College, Korukkai, Thiruvavur(Dt)-614711, punithajdd2012@gmail.com

^{*}Associate Professor, Department of Chemistry, Annamalai University, Annamalai Nagar 608 002, India

a Corresponding author

Dr. P.PUNITHA
Assistant Professor
Department of Chemistry,
Government Polytechnic College,
Korukkai, Thiruvavur (Dt)-614711.

ABSTRACT

The effect of the addition of Se (IV) on the growth and various properties of ammonium di hydrogen phosphate single crystals grown from aqueous solution by the slow evaporation method have been studied. The grown crystals were subjected to FT-IR, UV-Vis TG/DTA, Powder XRD, SEM-EDS and NLO studies. The reduction in the intensity observed in powder X-ray diffraction of doped specimen and The FT-IR spectral analysis confirms that slight shifts in vibrational frequencies confirm the lattice stress as a result of doping. UV-Vis study shows that the transparency is not affected much by the dopants. Thermal analysis studies reveal the purity of the materials and no decomposition is observed up to the melting point The reduction in the intensity observed in powder X-ray diffraction of doped specimen. Surface morphological changes due to doping of selenium metal are observed by scanning electron microscopy. The incorporation of Se(IV) in to the crystal lattice was confirmed by energy dispersive X-ray spectroscopy. The crystal is further characterized by Kurtz powder technique and Non-Linear optical studies.

Keywords: Non-Linear Optics, Characterisation, Growth from solution, X-diffraction, Selenium Compounds, Crystal growth; Spectral analysis.

1. Introduction

Non-Linear Optical materials capable of efficient second harmonic generation have been actively sought over the last three decades due to commercial importance of these materials in the fields of optical communication, single processing (1). The demand for large-Size ADP and KDP-type single crystals has increased sharply in recent years because of these crystals have important Piezoelectric, Ferroelectric, Electro-optic and Non-linear Optical properties (2-5). Such demand requires the rapid growth of crystal in a

shorter duration of time while maintaining the quality and size. The contents of impurities in the raw materials are important factors for the rapid growth of crystals. The capture of an impurity in a crystal during its growth from solution is a combined effect of various factors such as solubility of host and the impurity phase, character of mother phase, interaction between the host and the impurity and host ions, similarity in the crystallographic structure to the two phases, relative size of the impurity and the host ions and other crystallization condition(6,7). KDP and ADP solutions always contain some unintentional impurities such as Fe^{3+} , Cr^{3+} and Al^{3+} have noticeable effects on growth rate, morphology and quality of ADP and KDP type crystals grown from aqueous solution. An impurity can suppress, enhance or stop the growth of crystal completely (8,9). The impurity effects depends on the impurity concentration and super saturation temperature and p^{H} of the solution. Some theoretical treatments have successfully explained the impurity effect on the crystal growth(10,11) Until now, the effect of these impurities on the crystallization process of the KDP and ADP type crystals has not been born out very clearly, so it is necessary to do further research(10). In our laboratory efforts were made to find the effects of tetravalent selenium ions on the growth and important properties of ammonium dihydrogen phosphate single crystals and the results are reported herein and discussed.

2. Experimental

2.1. Synthesis and crystal growth

Equimolar concentration of the components ammonium dihydrogen phosphate and selenium dioxide were dissolved in triply distilled water and thoroughly mixed for 3 hours using a magnetic stirrer to ensure the homogeneity of the solution. The solution was covered with perforated paper and left undisturbed. The crystals were grown from slow evaporation solution growth technique. Good quality bulk crystals were harvested in a period of 3 weeks. It is shown in (Fig.1).



Fig.1. Photograph of ADP crystals (A) pure and (B) Se doped crystal

2.2. Characterization technique

The Fourier transform infrared (FT-IR) spectra were recorded using Avatar 330 FT-IR by the KBr pellet technique. The UV-Vis absorption spectra were recorded by using a Hitachi UV-Vis spectrophotometer in the spectral range 200–800 nm for all the samples. The powder X-ray diffraction was performed by using a Philips Xpert Pro Triple-axis X-ray diffractometer at room temperature using a wavelength of 1.54 Å and a step size of 0.008°. The samples were examined with Cu-K α radiation in a 2 θ range of 10 to 70°. The XRD data were analyzed by the Rietveld method with RIETAN-2000 (12). Surface Morphology of the samples and the presence of dopants in the specimens were observed by using JEOL JSM 5610 LV scanning electron microscope with a resolution of 3.0 nm, an accelerating voltage of 20 kV and a maximum magnification of 300,000 times. In order to know the thermal stability of the grown crystals thermogravimetric(TGA) and differential thermal analysis (DTA) were performed using Perkin Elmer Diamond TG-DTA thermal analyzer at heating rate 20 °C min⁻¹ ranging from 0–800 °C at inert nitrogen atmosphere. The SHG efficiency of the specimens was measured by the Kurtz powder method (13).

3. Results and discussion

3.1. FT-IR spectral analysis

The infrared spectral analysis was carried out to understand the chemical bonding and it provides useful information regarding the molecular structure of the compound. FT-IR spectra were recorded for as-grown crystal in the range of 400-4000 cm^{-1} (Fig.2).

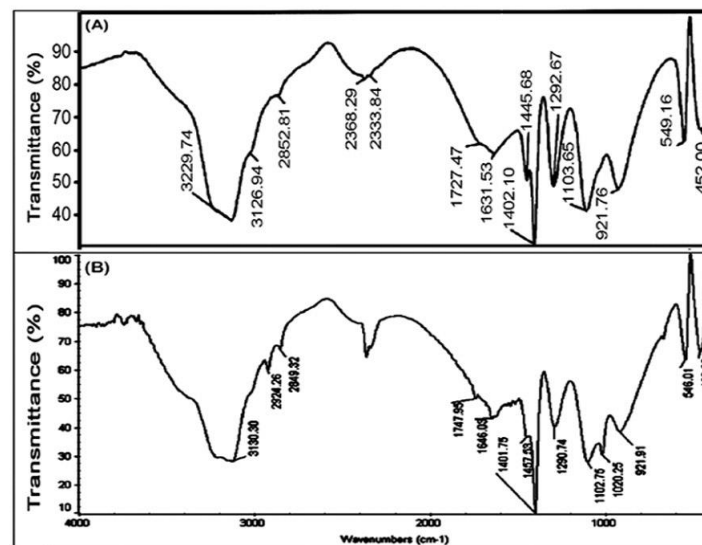


Fig.2 FT-IR spectra of ADP crystals: (A) pure and (B) Se doped crystal

A close observation of FT-IR spectra of pure and doped specimens reveal the doping generally results in small shifts in some of the characteristic vibrational frequencies. It could be due to lattice strain developed as result of doping. FT-IR spectrum of pure and the Se -doped ADP as shown in Table.(1). The Broad peak at 3250 cm^{-1} due to O-H vibration also P-O-H and N-H vibration for pure ADP is shifted to 3130 cm^{-1} in selenium doped ADP. But, the peaks 1706, 1642 cm^{-1} due to O-H bending vibration in pure ADP were shifted to 1747 cm^{-1} and 1646 cm^{-1} respectively due to the effect of Selenium. The P-O-H vibration peaks at 1092 cm^{-1} and 910 cm^{-1} in parent ADP were shifted to 1102 cm^{-1} and 921 cm^{-1} in Selenium doped ADP .

Table 1

Vibrational frequencies (cm^{-1}) for pure ADP and Se doped ADP crystals.

Pure ADP	Se doped ADP	Assignment
3126	3130	O-H stretching
2852	2849	N-H stretching NH_4
1402	1401	Bend stretching of NH_4
1292	1290	Combination band of stretching
1103	1102	P-O-H stretching
549	546	PO_4 stretching
452	462	PO_4 stretching

3.2. UV-Vis absorption spectra

The optical absorption spectrum of the grown crystal was recorded in the wavelength range between 200-400nm using Perkin-Elmer lambda 25 UV-spectrometer and the resultant spectrum is shown in Fig.(3). The crystal is transparent in the entire visible region and UV cutoff wavelength is found to be at 350nm. The very low absorption in the entire visible region confirms its suitability for the fabrication of non-linear optical devices. The measurement of the absorption coefficient α as a function of frequency ν of the incident beam provides a mean to determine the band gap E_g of a material. The optical band gap in most of the materials can be determined using the Tauc relation, which is expressed as

$$(\alpha h\nu) = A(h\nu - E_g)^r$$

Where 'A' is a constant and r is an index which depends on the nature of electronic transition responsible for the optical absorption.

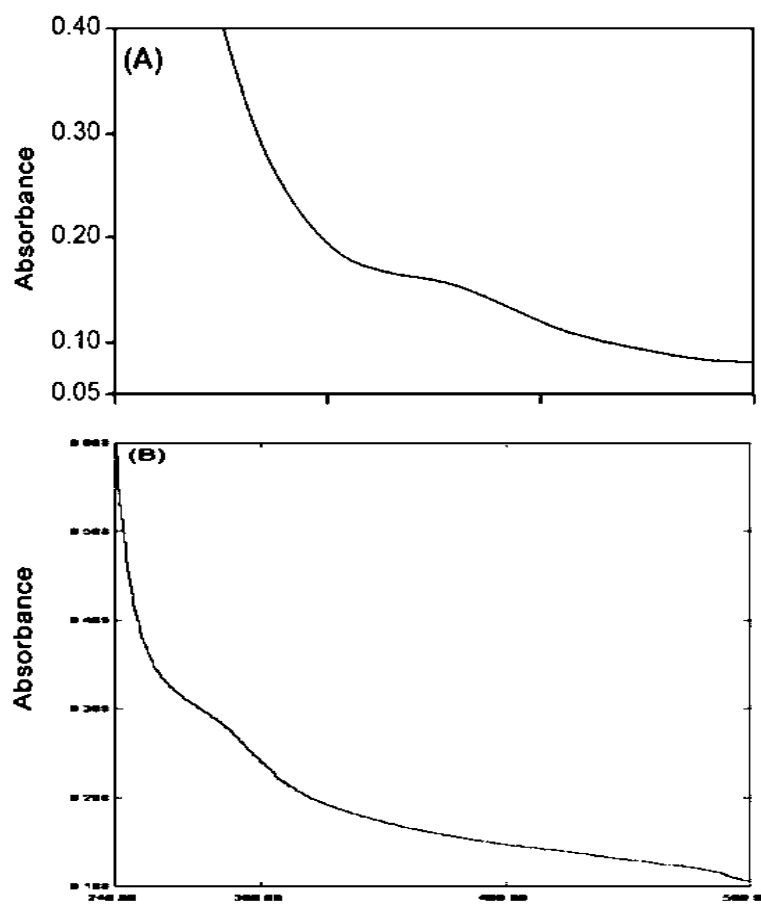


Fig. 3. UV-Vis spectra of ADP crystals: (A) pure and (B) Se doped crystal

Tauc's plot of the optical absorption spectrum measured at room temperature for Se-doped and undoped ADP are given in (Fig.4). The direct optical energy gap can be obtained from the intercept of the resulting

straight lines with the energy axis at $(\alpha h\nu)^2=0$ and the band gap for pure and Se(IV) doped ADP crystals are 5.5 and 5.8 eV. It is interesting to observe that the doping results in increase in band gap energy of the host material.

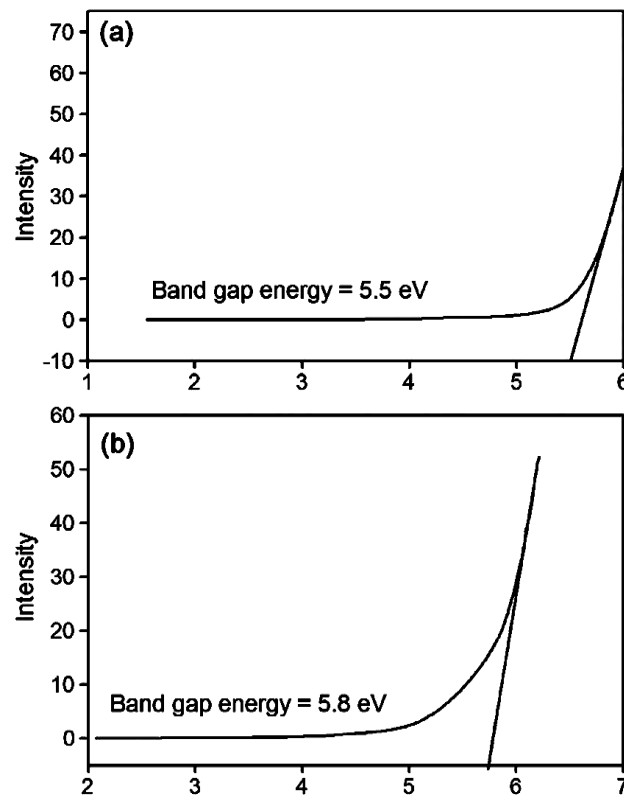


Fig. 4. Band gap energy of ADP crystals: (A) pure and (B) Se doped crystal

3.3. Powder X-ray diffraction

Powder X-ray diffraction (XRD) pattern of pure ADP crystals are compared with doped ADP crystals as shown in Fig.(5). Powder XRD patterns indicate that the formed crystals are in the single phase with good crystalline nature. XRD patterns of Se- doped samples are similar to pure ADP and no change from the basic structure of ADP is observed. General observation is intensity reduction and slight shift in the peak positions for doped sample, which could be due to the occupation of dopant in the host crystal of ADP. Average dimension of crystallites (t) are calculated using Scherrer equation (15).

$$t = \frac{K\lambda}{(\beta \cos \theta)}$$

Where K is Scherrer constant; λ is the wavelength of X-ray, θ is the peak position measured in radian and β is the integral breadth of reflections located at 2θ . The granularity of the crystal decreases from 79 to 76 nm by doping. It appears that the doping does not inhibit the growth of the crystal. The ionic radius of the dopant Selenium (66pm) is small compared with that of ammonium ion (143 pm) and hence it is reasonable

to believe that selenium occupies predominantly substitutional positions. However, the lattice parameter values obtained using single crystal XRD (Table.2) indicates that there is no new compound formation as the crystal system and the a,b,and c values are same(16).The lattice parameter values of pure and doped crystals are listed in (Table.2)A small change in the c-axis value of doped samples when compared with the pure ADP is attributed to strains in the lattice because of doping .Interstitial occupancy of dopant and partial substitution as in the case of ADP and KDP mixed crystal (17) are also not ruled out.

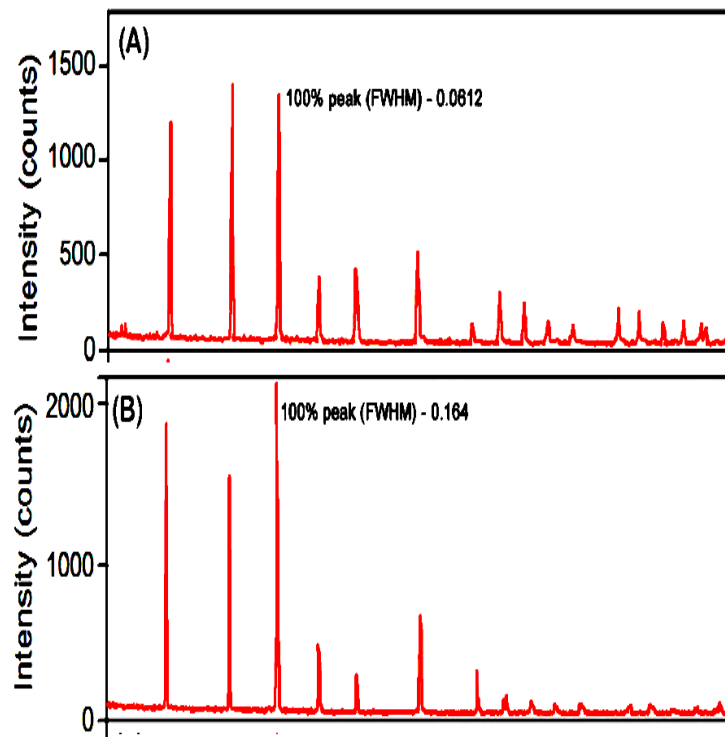


Fig.5. XRD patterns of ADP crystals: (A) pure and (B) Se doped crystal

Table 2

Lattice parameter values for pure ADP and Se doped crystals.

Crystal	$a=b$ (Å)	c (Å)	V (Å ³)	System
Pure ADP	7.502	7.566	428.6	Tetragonal
ADP doped Se	7.459	7.459	423.0	Tetragonal

3.4. SEM-EDS analysis

Scanning electron microscope study gives information about the surface nature and its suitability for device fabrication. It is also used to check the presence of imperfections (Fig.6) shows the scanning electron micrographs recorded for the ADP single crystal specimens. The micrograph (a) depicts the surface features of undoped specimen and shows a reasonably good uniform surface with some roughness, probably due to impurities. The picture (b) is of Se-doped ADP crystal in its as-grown state. The micrograph suggests that

the specimen has a plate morphology due to dopants. The incorporation of Se in to the crystalline matrix was confirmed by EDS performed on ADP.

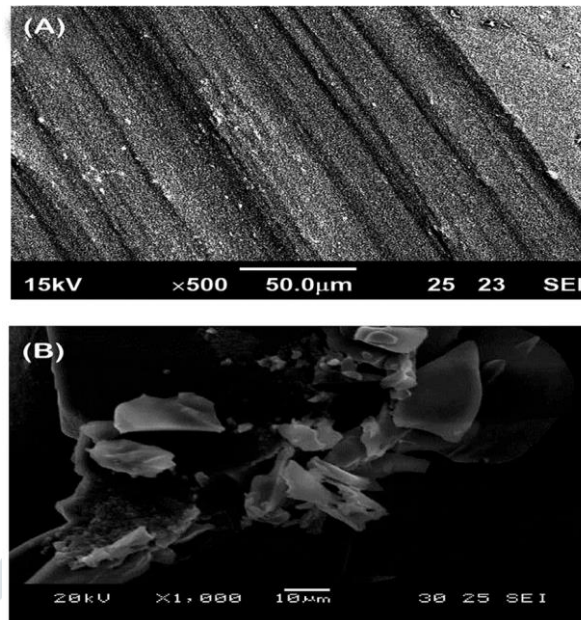


Fig.6. SEM images of ADP crystals: (A) pure (layered like structure) and (B) Se doped crystal

It appears that the accommodating capability of the host crystal is limited and only a small quantity is incorporated in to the ADP crystalline matrix. Further, analysis of the surface at different sites indicates that the incorporation is non-uniform over the surface, connected with adsorption mechanisms. EDS spectra reveal that the accommodating capability of ADP is better as shown in Fig(7).

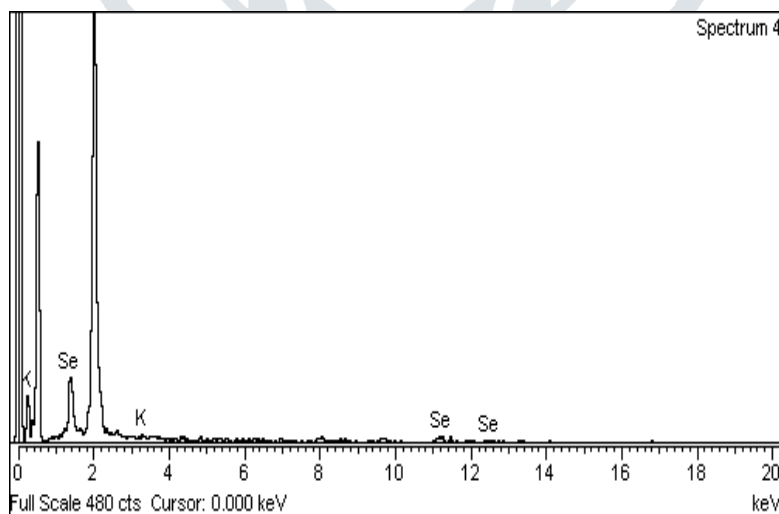


Fig.7. EDS of Se doped ADP crystal

3.5. TGA-DTA analysis

The thermal analysis was used to find out the weight loss percentage using Thermo Gravimetric Analysis and Differential Thermal Analysis in the sample with temperature. In the present study, thermal analysis has been carried out on the grown materials using Perkin Elmer Thermal Analysis STA 6000 temperature scan between the temperatures from 0°C to 600°C at a heating rate of 15°C/min in N₂ ambient. The recorded spectrum of Se doped ADP crystal is shown in Fig (8). From the TGA curve, it is clearly noted that the material is very stable and there is no phase transition up to 180°C. The absence of water of crystallization in the molecular structure is indicated by the absence of weight loss around 100°C. It is found that weight loss occurred there is a sharp endothermic peak at 199°C. Which is assigned to the melting point of the specimen but below this temperature no peak is observed which illustrates the absence of any isomorphous transition. No decomposition up to the melting ensures the suitability of the material for application in lasers where the crystals are required to withstand high temperature is observed in DTA curve shows a good degree of crystallinity of the sample. This melting point is relatively higher in comparison with the parent crystal.

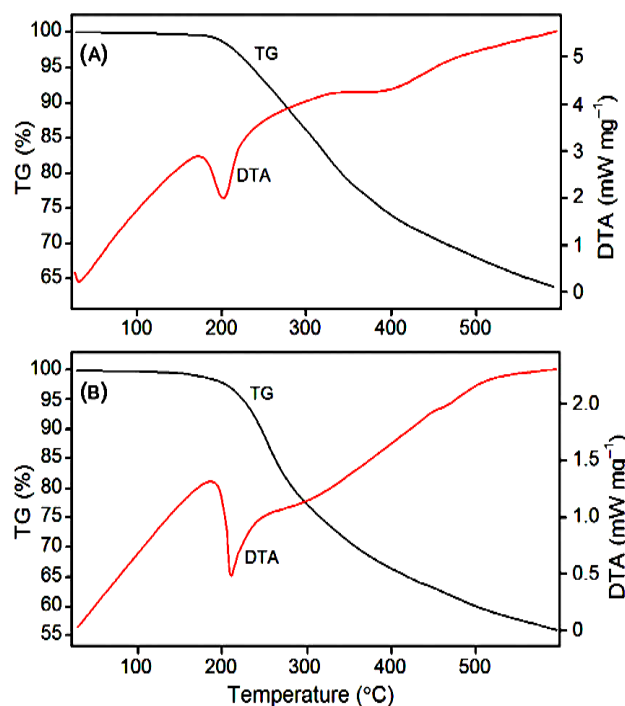


Fig. 8. TG-DTA curves of ADP crystals: (A) pure and (B) Se doped crystal

3.6. SHG analysis

The most widely used techniques for confirming the SHG efficiency of NLO materials to identify the materials with non-Centrosymmetric crystal structure in the Kurtz powder technique [12]. A Q-switched

Nd:YAG laser beam of wavelength 1064 nm was used with an input power at 2.5 mJ pulse. Many materials have been identified that have higher molecular non-linearities, the attainment of second order effects requires favorable alignment of molecule within the crystal structure. The efficient SHG demands specific molecular alignment of crystals to be achieved facilitating nonlinearity in the presence of dopant. It has been reported that SHG can be greatly enhanced by altering molecular alignment through inclusion complexation(18).

It is interesting to observe that the addition of Selenium enhance the SHG efficiency of ADP in Table.(3).Se(IV) doping significantly improves the non-linear optical property and hence it is a useful dopant.

Table 3

SHG output.

System	$I_{2\omega}$ (mV)
Pure ADP	11.6
ADP doped Se	18.0

4. Conclusions

Effect of doping the Se(IV) on the ADP crystals has been studied. FT-IR spectra indicate that doping has not altered the basic structure of ADP. Transparency of the doped crystal has not affected in the UV-Vis studies. Thermal studies reveal the doping of ADP leads to an increase in the decomposition temperature when compared to the pure ADP crystal. Powder XRD studies implies the crystalline nature of the sample. The facts that no appreciable change in the lattice parameter values and crystal system of doped sample indicate the unchanged crystal structure of pure ADP as revealed in the single crystal XRD analysis. SEM images reveal that the external morphology of ADP crystal is changed by doping. EDS studies reveals the incorporation of Se(IV) in the crystalline matrix of ADP crystals. It is interesting to observe the doping of selenium enhances the second harmonic generation efficiency. Hence Se doping can be utilized for optoelectronic application of ADP. Increased SHG value in the case of doped ADP could be due to unfavourable molecule alignment.

References

[1] A. Yokotani, T. Sasaki, K. Yamanaka, Ch. Yamanaka, Appl. Phys. Lett. 48 (1986) 1030.

- [2] J.D. Lindl, Phys. Plasmas (1955) 2.
- [3] D. Eimerl, Ferroelectrics 72 (1987) 95.
- [4] H. Tukubo, H. Makita, J. Crystal Growth 94 (1989) 469.
- [5] L. Glasser, Chem. Rev. 75 (1975) 21.
- [6] M.J. Gunning, R.E. Raab, W. Kucharczyk, J. Opt. Soc. Am. B18 (2001) 1092.
- [7] R.W.G. Wyckoff, Crystal Structures, 2nd ed., Interscience, New York, 1960, p.160.
- [8] A. Abdel-Kader, J. Mater. Sci. Mater. Electron. 2 (1991) 7.
- [9] N. Peeresy, M. Souhassouy, B. Wynckey, G. Avoilleyx, A. Coussonzand, J. Phys.: Condens. Matter 9 (1997) 6555.
- [10] R.J. Davey, J.W. Mullin, J. Cryst. Growth 26 (1974) 45.
- [11] R.I. Ristic, J.N. Sherwood, J. Phys. D: Appl. Phys. 24 (1991) 171.
- [12] A. Boujhris, M. Souhassou, C. Lecomte, B. Wyneke, A. Thalal, J. Phys.: Condens. Matter 10 (1998) 1621.
- [13] J.W. Mullin, Crystallization, 3rd ed., Butterworth Heinemann, London, 1993.
- [14] L.N. Rashkovich, N.V. Kronsny, J. Cryst. Growth 182 (1997) 434.
- [15] G. Bhagavannarayana, S. Parthiban, S.P. Meenakshisundaram, J. Appl. Crystallogr. 39 (2006) 784.
- [16] V.A. Kuznetsov, T.M. Okhrimenko, M. Rak, SPIE Proc. 3178 (1997) 100.
- [17] G. Li, L. Xue, G. Su, Z. Li, X. Zhuang, H. Ha, Cryst. Res. Technol. 40 (2005) 867.
- [18] J. Podder, S. Ramalingom, S. Narayanakalkura, Cryst. Res. Technol. 36 (2001) 549.
19. F. Izumi and T. Ikeda, Mater. Sci. Forum, 2000, 321–324, 198–203.
20. S.K. Kurtz, T.T. Perry, Journal of Applied Physics 39 (1968) 3798–3813.
21. A.L. Patterson, Phys. Rev. 56 (1939) 978–982.
22. Amutha M, Ramasamy G, Meenakshisundaram SP, Mojumdar SC. Effect of s-, p-, d-, and f-block elements on the structure and properties of ammonium dihydrogen phosphate crystals. J Therm Anal Calorim. 2011;104:949–54.
23. Parthiban S, Meenakshisundaram S. Synthesis, crystal structure and NLO properties of a mixed crystal $K_{1-x}(NH_4)_xH_2PO_4$ ($x = 0.5$). J Chem Crystallogr. 2011;41:111–4.

Captions for figures

Fig. 1. Photograph of Se doped crystal.

Fig. 2. FT-IR spectra of (a) ADP and (b) Se doped crystals.

Fig. 3. UV-Vis spectrum of pure and Se doped crystals.

Fig. 4. Band gap energy of pure and Se doped crystals.

Fig. 5. SEM image of pure and Se doped crystals.

Fig. 6. EDS of Se doped crystal.

Fig. 7. TG-DTA curves of pure and Se doped crystals.

Fig. 8. XRD patterns of pure and Se doped crystals.

